Available online at www.sciencedirect.com
SCIENCE DIRECT®
Bioorganic & Medicinal Chemistry 13 (2005) 1867–1872
Bioorganic & Medicinal Chemistry

Cell adhesion inhibitory activity of (*d*)-corynoline, a hexahydrobenzo[*c*]phenanthridine-type alkaloid, and its structure–activity relationship, studied by X-ray crystal structure analysis and molecular docking study

Miyoko Kamigauchi,[a,*] Yuko Noda,[a] Jujiro Nishijo,[a] Katsuhide Iwasaki,[b] Kenji Tobetto,[b] Yasuko In,[c] Koji Tomoo[c] and Toshimasa Ishida[c]

[a]*Department of Physical Chemistry, Kobe Pharmaceutical University, 4-19-1 Motoyama-kitamachi, Higashinada-ku, Kobe 658-8558, Japan*
[b]*MARUHO Co., Ltd Research and Development Laboratories, Kyoto 600-8815, Japan*
[c]*Osaka University of Pharmaceutical Sciences, 4-20-1 Nasahara, Takatsuki Osaka 569-1094, Japan*

Received 6 August 2004; revised 19 October 2004; accepted 21 October 2004
Available online 25 December 2004

Abstract—Corynoline (**1**), a hexahydrobenzo[*c*]phenanthridine-type alkaloid, exhibited the concentration-dependent inhibition for the adhesion of human polymorphonuclear leukocyte and eosinophil to human umbilical vein cultured endothelial cell in the concentration range of showing no significant cytotoxicity for the cell: IC_{50} value = 72.4 μM for (*d*)-**1** and 156.7 μM for (*l*)-**1**. This shows the potent anti-inflammatory and/or immunosuppressive activity of **1**. To elucidate possible structure–activity relationship, the conformational/structural feature of (*d*)-**1** was investigated by X-ray crystal structure analysis and molecular orbital energy calculations, and the docking study was performed for its interaction with the D1-domain of ICAM-1 (intracellular adhesion molecule-1). A plausible model was proposed, in which all polar atoms of (*d*)-**1** are linked by hydrogen bonds or electrostatic interactions with the functional residues of ICAM-1, that have been supposed to be necessary for the binding with LFA-1 (leukocyte function-associated antigen-1). This suggests the potent inhibitory activity of **1** for the ICAM-1/LFA-1 adhesion and would be important on developing the clinically usable drugs for the inflammatory diseases.

1. Introduction

Leukocyte adhesion to vascular endothelial cells is an essential step in the development of inflammatory diseases.[1,2] It is now well known that the adhesion of leukocytes to endothelial cells can be stimulated by factors acting on the adhesiveness of the leukocytes or endothelial cells.[3–5] We have searched for inhibitors of leukocyte–endothelial cell adhesion, which could be used as anti-inflammatory drugs. The following two processes are indispensable for the formation of inflammation, that is (i) the rolling of leukocyte on vascular endothelial cells[6] and (ii) the adhesive interaction of leukocyte with the vascular endothelial cells[7] (Fig. 1). It is well known that various adhesive molecules.[8] such as selectin family (ELAM-1), integrin family (LFA-1, Mac-1, etc.), and immunoglobulin superfamily (ICAM-1, VCAM-1, etc.),[9,10] are concerned with the adhesions of T-cell, antigen presentation cell, cancer cell, vascular endothelial cell, and so on. All of these molecules function on cell surface and fulfill their important roles in the immunological reaction and cancer metastasis. Therefore, it could be expected that the molecules to inhibit such cell adhesion are useful as a therapeutic agent for the inflammation and allergy, autoimmune disease, and cancer. Although the monoclonal antibody of each adhesive molecule has already been shown to be effective,[11,12] it also causes serious problems such as the side effect based on the antigenicity. In order to solve this problem, therefore, it has been desired the development of the low-molecular weight inhibitors.

Keywords: Corynoline; Alkaloid; Cell adhesion inhibitory activity; Structure–activity relationship.
* Corresponding author. Tel.: +81 78 441 7540; fax: +81 78 441 7541; e-mail: kamigami@kobepharma-u.ac.jp

0968-0896/$ - see front matter © 2004 Elsevier Ltd. All rights reserved.
doi:10.1016/j.bmc.2004.10.065

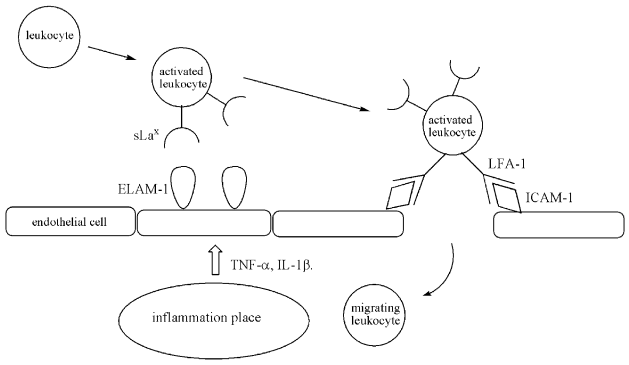

Figure 1. Adhesion step in the inflammatory reaction between leukocyte and endothelial cell. The leukocytes and vascular endothelial cells are activated by the inflammatory cytokine (TNF-α, Il-1β, etc.) during (i) the rolling stage of the leukocyte through the selectin molecule (ELAM-1) and its ligand (sLa^x), (ii) the adhesion stage of the leukocyte through the integrin molecule (LFA-1) and its ligand (ICAM-1), and (iii) the transmigrating stage of the leukocyte to the inflammation position.

Corynoline (**1**, Fig. 2) is a representative hexahydrobenzo[*c*]phenanthridine-type alkaloid of traditional folk medicinal plant *Corydalis incisa* (papaveraceae). As a series of developing the clinical-usable medicine from the natural plants, we have been investigating the structural analyses, biosyntheses, metabolisms, and bioactivities of phenanthridine-type alkaloids because of their major components of medical plants commonly used in Chinese and natural medicine.[13–18] In this paper, we report the cell adhesion inhibitory activity of **1.** To elucidate its structure–activity relationship, furthermore, the conformational/structural stability of (*d*)-**1** enantiomer was investigated by the X-ray crystal structure analysis and the molecular orbital energy calculations, and a plausible docking model was proposed for the interaction of **1** stable conformation with the D1-domain of ICAM-1 (intracellular adhesion molecule-1).

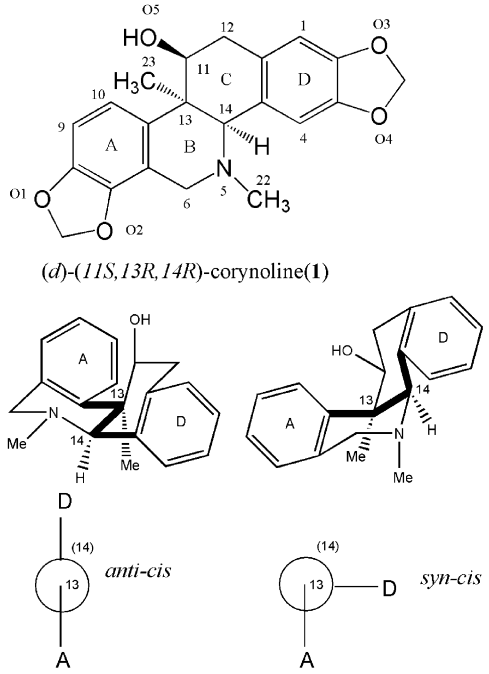

Figure 2. Chemical structure of **1**, together with atomic numbering used in this work, and *anti-cis* and *syn-cis* conformations by Newman projection from C13 to C14 of hexahydorbenzo[*c*]phenanthridine skeleton.

2. Results and discussion

2.1. Cell adhesion inhibitory effect and cytotoxicity

The adhesion depression effect of (*dl*)-**1** on human polymorphonuclear leukocyte (PMNL) to human umbilical vein cultured endothelial cell (HUVEC) was examined in a static adhesion assay according to the method of Utoguchi et al.,[19] where HUVEC was activated by IL (interleukin)-1β and PMNL was labeled with fluorescent dye BCECF (2′,7′-bis-(2-carboxyethyl)-5-(and-6)-carboxyfluorescein), to determine the concentration. As a result, **1** was shown to suppress the adhesion between PMNL and HUVEC in a concentration-dependent manner (Fig. 3a); the inhibition was IC_{50} = 54.8 μM. On the other hand, since the neutrophil adhesion to HUVEC would be inhibited if **1** were toxic to PMNL and HUVEC, LDH (lactate dehydrogenase) activities in HUVEC and PMNL-conditioned mediums were measured as an index of cytotoxicity of **1** (Table 1). The results showed that the activity level is not significantly different from that of control. Therefore, it is concluded that the toxicity of **1** to HUVEC and PMNL during 24 h incubation is almost negligible and any impairment for the cell is not recognized in this concentration range.

To clarify the adhesion depression effect of **1** optical isomers, the actions of both (*d*)- and (*l*)-**1** to HUVEC were examined for the adhesion of eosinophil (EoL-1),[20] which is one of leukocytes and participates in the pathogenesis of allergic diseases. The result is shown in Figure 3b, where the inhibition was IC_{50} = 38.4 μM for (*d*)-**1** and 71.2 μM for (*l*)-**1**. Although the direct comparison between Figure 3a and b is not possible because of the different experimental system, it is obvious that the activity of (*d*)-**1** has the most active concentration-dependent cell adhesion inhibitory activity.

To clarify the functional point of **1** for its adhesion inhibitory activity, the inhibition rates for the TNF-α- and IL-1β-induced expressions of adhesive proteins ELAM-1, ICAM-1, and VCAM-1 were estimated by direct cell ELISA assay (Table 2). The results suggested that the activity of **1** is revealed by the adhesion inhibition of the integrin family with ICAM-1/VCAM-1, not by the inhibition of biological function of ELAM-1.

2.2. X-ray crystal structure analysis of (*d*)-1

Concerning the molecular conformation of the *cis*-fused B/C ring moiety of the hexahydrobenzo[*c*]phenanthridine type alkaloid (Fig. 2), there are two types, *anti-cis* and *syn-cis*,[16] because the B/C ring junction moiety

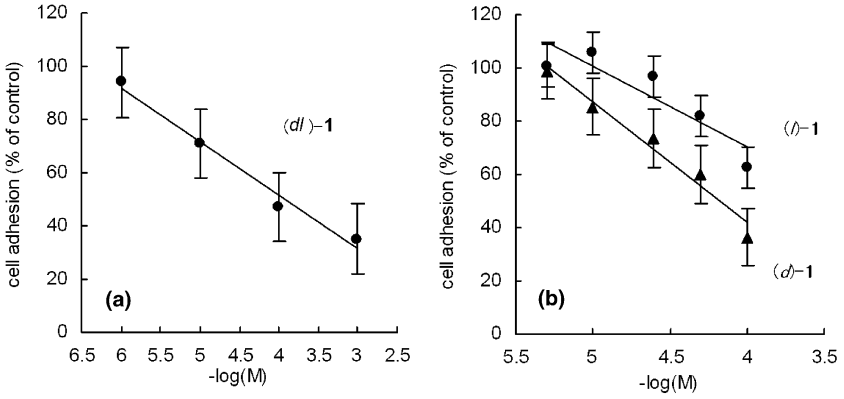

Figure 3. (a) Effects of (*dl*)-**1** for PMNC adhesion to IL-1β-stimulated HUVEC. Confluent HUVEC monolayers were incubated with IL-1β (200 U/mL) for 4 h at 37 °C and washed by **1** for 30 min prior to the addition of BCECF-labeled PMNC (4×10^5 cells/cm^2) and then subjected to the PMNC-monolayer adhesion assay. Assays were run in triplicate for each dilution. Error bars represent the standard error. (b) Effects of (*d*)- and (*l*)-**1** for EoL-1 adhesion to TNF α-stimulated HUVEC. Confluent HUVEC monolayers were incubated with TNFα (200 U/mL) for 24 h at 37 °C and washed by each alkaloid for 30 min prior to the addition of BCECF-labeled EoL-1s (4×10^5 cells/cm^2) and then subjected to the EoL-1-monolayer adhesion assay. Assays were run in triplicate for each dilution. Error bars represent the standard error.

Table 1. The inhibition of (*dl*)-**1** against the HUVEC and PMNL viability[a]

(*dl*)-**1** concentration(M)	HUVEC LDH (%)	PMNL LDH (%)
10^{-6}	1.5	0.3
10^{-5}	−1.4	−0.4
10^{-4}	−4.8	−0.6

[a] HUVEC and PMNL were incubated for 24 h at 37 °C in the absence (control) and presence of (*dl*)-**1** at the indicated concentration. The cell inhibitory was determined by the LDH assay.

Table 2. The inhibition of (*dl*)-**1** against the IL-1β- and TNFα-stimulated expression of ELAM-1, ICAM-1, and VCAM-1

	Inhibition rate (%)
IL-1β-stimulated ICAM-1	52
IL-1β-stimulated ELAM-1	~0
TNFα-stimulated ICAM-1	44
TNFα-stimulated ELAM-1	~0
TNFα-stimulated VCAM-1	72

IL-1β or TNFα was incubated with HUVEC for 24 h at 37 °C in the absence (control) and presence of (*dl*)-**1**. The concentration of (*dl*)-**1** was kept at 100 μM. The expression of ELAM-1, ICAM-1, or VCAM-1 was determined by the ELISA assay. Using the mouse monoclonal antibody for each adhesion molecule as the first antibody and the biotin-labeled anti mouse IgG antibody as the secondary antibody, the cell ELISA assay was performed using streptoavidine-binding alkaline phosphatase, and the inhibition rate was estimated from the absorbance measured by the ELISA assay.

could be flexible. It was shown by its crystal structure analysis[15] that (*dl*)-**1** takes an *anti-cis* type. The physicochemical data of the crystals of (*dl*)-**1** and (*d*)-**1** were considerably different concerning their melting points and crystal densities: 164° and 1.36 g cm^{-3} for (*d*)-**1** and 216° and 1.41 g cm^{-3} for (*dl*)-**1**. Therefore, it is interesting to examine the conformation of (*d*)-**1**, in addition to the elucidation of possible structure–activity relationship of **1** for its adhesion inhibitory activity. The absolute configuration of (*d*)-**1** has already been clarified by the chemical relation.[14]

The conformational feature was investigated by the X-ray crystal structure analysis. The X-ray data collections were carried out for both (*d*)-**1** and (*l*)-**1**. Consequently, the crystals of (*l*)-**1** showed the same crystallographic data, indicating the molecular/crystal packing is completely the same as (*d*)-**1**, except for the reverse absolute configuration. Thus, the X-ray crystal analysis was performed only for (*d*)-**1**, and the crystallographic data are given in Table 3; those of (*dl*)-**1**[15] were also given for comparison. The crystals of (*d*)-**1** contained three

Table 3. Summary of crystal data and details of intensity collection of (*d*)-**1**

	(*d*)-**1**	(*dl*)-**1**
Formula	$C_{21}H_{21}NO_5$	$C_{21}H_{21}NO_5$
Mr	367.4	367.4
Crystal system	Orthorhombic	Monoclinic
Space group	$P2_12_12_1$	P-1
a, Å	12.037(2)	12.639(2)
b, Å	53.307(8)	9.960(1)
c, Å	8.050(1)	7.490(1)
α, °	90.00	101.89(1)
β, °	90.00	101.74(1)
γ, °	90.00	78.29(1)
V, Å^3	5165(1)	865.6(5)
Z	12	4
D_x, g cm^{-3}	1.359(4)	1.409(4)
μ(CuKα), mm^{-1}	0.101	
F(000)	2328	
T of data collection, K	120	
Data range measured	$-15 < h < 16$, $-70 < k < 56$, $0 < l < 9$	
θ_{max}, °	28.91	
No. of independent reflections	12,431	
No. of observed reflections	11,568	
Criterion for observe reflections	$I > 2\sigma(I)$	
No. of parameters	730	
Goodness of fit	1.204	
R ; Rw for $I > 2\sigma(I)$	0.066; 0.142	
R ; Rw for all reflections	0.071; 0.144	
Mean shift/esd	0.001	
Flack χ parameter	0.0(8)	

crystallographically independent molecules (conformers I, II, III). Characteristically, three conformers took essentially the same conformation. The conformational features of (*d*)-**1** commonly observed in three conformers are as follows: the rings B and C take *twist-half-chair* and *half-chair* conformations, respectively, and the B/C ring junction is *anti-cis* conformation; the crystal of (*dl*)-**1** showed the essentially same conformation.[15] The *cis* B/C-form makes possible the formation of a six-membered intramolecular hydrogen bond between the axial-oriented hydroxyl O5H and the lone-paired electrons of N5:O···N5 = 2.719(3) Å for conformer I, 2.715(3) Å for II, and 2.693(3) Å for III. Interestingly, this value was significantly shorter than 2.885 Å of (*dl*)-**1**.[15] The volume calculation by the PM3 method (MOPAC software) according to its standard protocol gave 302 Å^3 for (*d*)-**1** and 308 Å^3 for (*dl*)-**1**. These data indicate that (*d*)-**1** takes a more compact conformation than (*dl*)-**1**. Thus, the different physicochemical data of (*dl*)-**1** and (*d*)-**1** crystals are due not to the different conformation of *cis*-fused B/C ring moiety, but to the different packing force.

In the (*dl*)-**1** and (*d*)-**1** crystals, crystal solvents were not contained and no intermolecular hydrogen bonds were formed. The respective molecules in both crystals were held by van der Waals forces among the neighboring molecules. However, their crystal densities and melting temperatures indicate the less stability of (*d*)-**1** crystal than (*dl*)-**1** crystal. This is due to the large free space that is required for the crystal packing of three crystallographically independent molecules in the (*d*)-**1** crystal (Fig. 4), as compared with that of one independent molecule in the (*dl*)-**1** crystal.

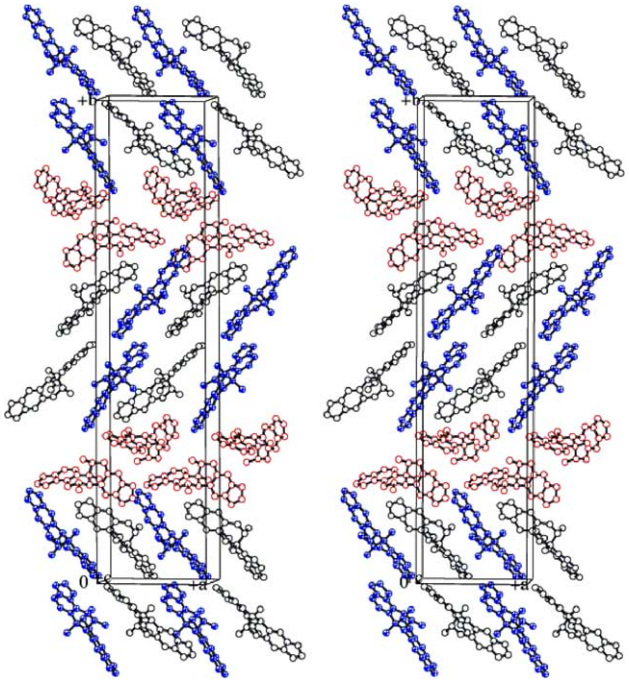

Figure 4. Stereoscopic view of crystal packing of (*d*)-**1**. The crystallographically independent three molecules (conformers I, II, and III) are marked by the black, red, and blue colors, respectively. The figure is projected from *c*-axis.

2.3. Docking study of (*d*)-1 on D1-domain of ICAM-1

In the inflammation, the leukocyte adhesion to vascular endothelial cells is an essential step and it occurs through the specific interaction between the integrin (LFA-1) and its ligand (ICAM-1).[21,22] Since the adhesion inhibitory activity of (*d*)-**1** could result from the inhibition of the specific LFA-1/ICAM-1 interaction, the possible binding of (*d*)-**1** to ICAM-1 was examined using the Docking module of Insight Discover, in which the binding at the D1-domain of ICAM-1 was considered, because its domain has been suggested to be important for the interaction with LFA-1.[23] Using the X-ray structure of the D1-domain of ICAM-1.[24,25] the docking site of (*d*)-**1** was surveyed so as to bind most stably to the D1-domain of ICAM-1 at the same site as for the I-domain of LFA-1; the docking study of RGD-containing cyclic peptide with D1-domain of ICAM-1 was also referred.[26] It was suggested that (*d*)-**1** preferentially binds to the C–D–E sheet and loop region of Glu34–Tyr52 sequence, because of many possible electrostatic and hydrogen bond formations. Consequently, a plausible interaction mode is shown in Figure 5. It is known that Glu34 in ICAM-1 is the most important residue for binding to LFA-1.[23] In this docking model of (*d*)-**1** to the D1-domain, a hydrogen bond formation is possible between the carboxyl O of Glu34 side chain and the O3 atom of (*d*)-**1**, if Glu34 residue is in a neutral form. And the O4 atom of (*d*)-**1** is linked by the hydrogen bond with N$^{\eta}$H group of Lys39 side chain, thus one of two methylenedioxy rings of (*d*)-**1** being tightly fixed by both Glu34 and Lys39 residues. On the other hand, the O2 atom of the other ring is also in the position of forming the hydrogen bond with the carboxyl O of Glu41 side chain, if the residue is in a neutral state, and the O1 atom forms a short contact with the carbonyl O of Asn47 side chain. The O5H group is hydrogen-bonded to the carbonyl O of Leu31 and forms a short contact with the N$^{\eta}$H group of Lys50 side chain. The N5 atom of (*d*)-**1** could be located at the position of forming an electrostatic interaction with the carboxyl O of Glu41 side chain and a hydrogen bond with O$^{\eta}$H of Tyr52 side chain.

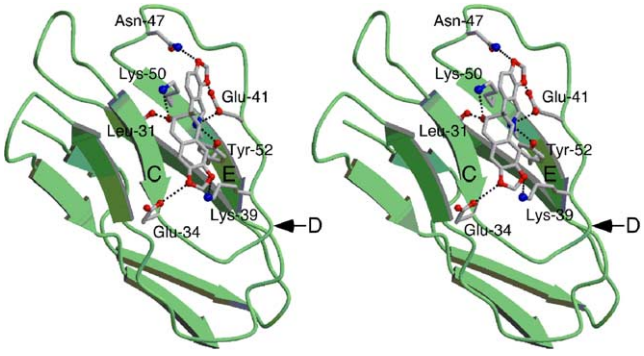

Figure 5. Stereoscopic view of possible docking of (*d*)-**1** (ball and stick model) on the D1-domain of ICAM-1 (green-colored ribbon model). The hydrogen bonds or electrostatic interactions are represented by dotted lines, respectively.

It appears important to note that this binding model is stereospecific, because the docking of (*l*)-**1** at the same site of ICAM-1 leads to a labile binding due to the breakage of interaction framework formed for (*d*)-**1**.

3. Conclusion

Corynoline (**1**) was clarified to show the concentration-dependent inhibition for the adhesion of PMNL and EoL to HUVEC in the concentration range, where **1** exhibits no notable cytotoxicity for HUVEC. The IC_{50} value was 72.4 μM for (*d*)-**1** and 156.7 μM for (*l*)-**1**, indicating the stereoselectivity of **1** for the adhesion inhibitory effect. To evaluate possible structure–activity relationship of **1**, the crystal structure of (*d*)-**1** was analyzed by X-ray diffraction method and clarified that **1** takes a rigid molecular conformation of the *twist-half-chair* and *half-chair* C rings and the *anti-cis* B/C ring junction; the different physicochemical property between the crystals of **1** racemate and optical isomer was shown to be primarily attributable to their crystal packing patterns. To investigate the structure–activity relationship of (*d*)-**1**, the docking study at the D1 domain of ICAM-1 was performed, and a plausible binding model was proposed, in which all polar atoms of (*d*)-**1** were linked with the functional residues of ICAM-1 with hydrogen bonds or electrostatic interactions. These results would be helpful when considering rational development of hexahydrobenzo[*c*]phenanthridine-type alkaloids in medical plants for the inflammatory diseases.

4. Experimental

4.1. Material

Compound (*dl*)-**1** was isolated from *C. incisa*, and (*d*)-and (*l*)-**1** were obtained by the optical resolution of (*dl*)-**1**.[14]

4.2. Assay

HUVEC were grown to confluence in 48-well plates coated with collagen and incubated for 4 h at 37 °C with and without IL-1β (200 U/mL) before washing. The cells were further incubated for 30 min at 37 °C with BCECF [2′,7′-bis-(2-carboxy-ethyl)-5-(and-6)-carboxy-fluorescein]-labeled PMNL (4×10^5 cells/well) in the presence of (*dl*)-**1** at an indicated concentration. After removal of non-adherent PMNL, its adhesion to HUVEC was determined by the measurement of fluorescence intensity. The remaining fluorescence intensity on HUVEC was measured by the dissolution of PMNL in the NaOH (0.1 M) aqueous solution including SDM (0.2%).

Confluent HUVEC monolayers were incubated with TNF-α (200 U/mL) for 24 h at 37 °C and washed prior to the addition of BCECF-labeled EoL-1s (4×10^5 cells/cm^2) and incubated with each of (*d*)- and (*l*)-**1** for a 30-min before the EoL-1-monolayer adhesion assay.

The inhibition of cell inhibitory was determined by the LDH assay. HUVEC (5×10^5 cells/mL) were incubated for 24 h at 37 °C in the absence (control) or presence of (*dl*)-**1** at an indicated concentration, and PMNL (5×10^5 cells/mL) were incubated for 4 h. Results: the mean ± SD ($n = 3$). The SD was all within ±0.5%.

4.3. X-Ray crystal analyses of (*d*)-1

Single crystal of (*d*)-**1** was crystallized from methanol/acetone at room temperature as transparent plates. A single crystal of dimensions of $0.4 \times 0.2 \times 0.15$ mm^3 was used for X-ray study. X-ray data were collected with a Bruker SMART APEX CCD camera using graphite-monochromated MoKα radiation ($\lambda = 0.71073$ Å) at 120 K. The crystallographic data are given in Table 3. The structure was solved by direct methods using the SHELXS-97 program.[27] The positional parameters of non-H atoms were refined by a full-matrix least-squares method with anisotropic thermal parameters using the program SHELXL-97.[28] The H positions of OH groups were all determined from a difference Fourier map, while those of other H-atoms were calculated on the basis of their stereochemical requirement. They were treated as riding with fixed isotropic displacement parameters ($U_{iso} = 1.2U$equiv for the associated C atoms, or $U_{iso} = 1.5U$equiv for methyl C or O atoms) and were not included as variables for the refinements. None of the positional parameters for non-H atoms shifted more than their estimated standard deviations, and the residual electron density in the final difference Fourier map were in the range of −0.318–0.391 e/Å^{-3}. The final atomic coordinates, anisotropic temperature factors, bond lengths, bond angles, torsion angles of non-H atoms, and the atomic coordinates of H atoms have been deposited in the Cambridge Crystallographic Data Center (CCDC 252839), Cambridge University Chemical Laboratory, Cambridge CB21EW.

4.4. Molecular orbital calculations

The molecular volumes of (*d*)- and (*dl*)-**1** were calculated on a 4D Indy using MOPAC Var.6 in MOL/MOLIS system.[29] The atomic coordinates from the X-ray crystal analyses were used for the calculations.

4.5. Docking study of (*d*)-1 to D1 domain of ICAM-1

The D1-domain (residues 1–83) coordinates for ICAM-1 were taken from the X-ray structure of the ICAM-1 D1-D2 domains from the Brookhaven Protein Data Bank (PDB code 1IC1). The atomic coordinate of conformer **1** of crystal structure of (*d*)-**1** was used for the docking studies. The possible docking site of (*d*)-**1** was surveyed onto the D1-domain of ICAM-1 using the Docking module of Insight Discover, where the rapid energy evaluation was performed for the reasonable configurational and transnational exploration.

References and notes

1. Osborn, L. *Cell* **1990**, *62*, 3.
2. Harlan, J. M. *Blood* **1985**, *65*, 513.

3. Barnes, P. J. *Am. J. Respr. Crit. Care Med.* **1994**, *150*, 42.
4. Humbert, M.; Ying, S.; Corrigan, C.; Menz, G.; Barkans, J.; Pfister, R.; Meng, Q.; Van Damme, J.; Opdenakker, G.; Durham, S. R.; Kay, A. B. *Am. J. Respir. Cell Mol. Biol.* **1997**, *16*, 1.
5. Collins, P. D.; Marleau, S.; Griffiths-Johnson, D. A.; Jose, P. J.; Williams, T. J. *J. Exp. Med.* **1995**, *182*, 1169.
6. Lawrence, M. B.; Springer, T. A. *Cell* **1991**, *65*, 859.
7. Walsh, G. M.; Symon, F. A.; Lazarovils, A. L.; Wardlaw, A. J. *Immunology* **1996**, *89*, 112.
8. Carlos, T. M.; Harlan, J. M. *Blood* **1994**, *84*, 2068.
9. Simmons, D.; Makgoba, M. W. *Nature Seed B* **1989**, *331*, 624.
10. Osborn, L.; Hession, C.; Tizard, R.; Vassallo, C.; Luhowskyj, S.; Chi-Rosso, G.; Lobb, R. *Cell* **1989**, *59*, 1203.
11. Mulligan, M. S.; Lentsch, A. B.; Shanley, T. P.; Miyasaka, M.; Johnson, K. J.; Ward, P. A. *Inflammation* **1998**, *22*, 403.
12. Von Andrian, U. H.; Chambers, J. D.; McEvoy, L. M.; Bargatze, R. F.; Arfors, K. E.; Butcher, E. C. *Proc. Natl. Acad. Sci. U.S.A.* **1991**, *88*, 7538.
13. Takao, N.; Iwasa, K.; Kamigauchi, M.; Sugiura, M. *Chem. Pharm. Bull. (Tokyo)* **1976**, *24*, 2859.
14. Takao, N.; Kamigauchi, M.; Iwasa, K. *Tetrahedron* **1979**, *35*, 1977.
15. Kamigauchi, M.; Noda, Y.; Takao, N.; Ishida, T.; Inoue, M. *Helv. Chim. Acta* **1986**, *69*, 1418.
16. Kamigauchi, M.; Miyamoto, Y.; Iwasa, K.; Takao, N.; Ishida, T.; In, Y.; Inoue, M. *Arch. Pharm. (Weinheim)* **1993**, *326*, 507.
17. Kamigauchi, M.; Noda, Y.; Iwasa, K.; Sugiura, M.; Nishijo, J.; In, Y.; Ishida, T. *J. Chem. Soc., Perkin Trans. 2* **1997**, 631.
18. Kamigauchi, M.; Yoshida, M.; Saiki, K.; Sugiura, M.; Nishijo, J.; In, Y.; Ishida, T. *Bull. Chem. Soc. Jpn.* **2000**, *73*, 1233.
19. Utoguchi, N.; Nakata, T.; Cheng, H. H.; Ikeda, K.; Makimoto, H.; Mu, Y.; Nakagawa, S.; Kobayashi, M.; Kitagawa, I.; Mayumi, T. *Inflammation* **1997**, *21*, 223.
20. Tominaga, T.; Watanabe, A.; Noma, S.; Tsuji, J.; Koda, A. *Allergol. Int.* **1996**, *45*, 91.
21. Springer, T. A. *Cell* **1994**, *76*, 301.
22. Springer, T. A. *Nature* **1990**, *346*, 425.
23. Staunton, D. E.; Dustin, M. L.; Erickson, H. P.; Springer, T. A. *Cell* **1990**, *61*, 243.
24. Bella, J.; Kolatkar, P. R.; Marlor, C. W.; Greve, J. M.; Rossmann, M. G. *Proc. Natl. Acad. Sci. U.S.A.* **1998**, *95*, 4140.
25. Casasnovas, J. M.; Stehle, T.; Liu, J. H.; Wang, J. H.; Springer, T. A. *Proc. Natl. Acad. Sci. U.S.A.* **1998**, *95*, 4134.
26. Xu, C. R.; Yusuf-Makagiansar, H.; Hu, Y.; Jois, S. D.; Siahaan, T. J. *J. Biomol. Struct. Dyn.* **2002**, *19*, 789.
27. Sheldrick, G. M. SHELXS97. Program for the Solution of Crystal Structure. University of Gottingen, Gottingen, Germany, 1997.
28. Sheldrick, G. M. SHELXL97. Program for the Refinement of Crystal Structures. University of Gottingen, Gottingen, Germany, 1997.
29. MOL/MOLIS; Molecular Orbital Analysis System. Daikin Industries, Ltd.